

# An Immobilised Silicon-Carbon Bond-Forming Enzyme for Anaerobic Flow Biocatalysis

Sabrina Gallus<sup>+, [a]</sup>, Esther Mittmann<sup>+, [a]</sup>, Annika J. Weber<sup>+, [a]</sup>, Martin Peng,<sup>[a]</sup>  
 Christof M. Niemeyer,<sup>[a]</sup> and Kersten S. Rabe<sup>\*[a]</sup>

The recent development of tailored cytochrome enzymes has enabled “new-to-nature” reactivities, such as the biocatalytic formation of carbon-silicon bonds using the cytochrome c from *Rhodothermus marinus*. To maximise the potential of this remarkable biocatalyst by increasing its turnover numbers (TON) and to enable its reusability in continuous processes, we report the use of the SpyTag/SpyCatcher bioconjugation system to immobilise this enzyme. We successfully modified the enzyme with a SpyTag without significant effects on its catalytic

activity. Even after immobilization on microparticles the enzyme retained 60% activity. When the immobilized enzyme was used in sequential batch or continuous flow to produce an organosilicon, we observed up to 6-fold higher turnover numbers over a total period of 10 days compared to the free enzyme reaction, however we observed a drop in stereoselectivity under these conditions. This is the first report on the successful immobilisation of a carbon-silicon bond forming enzyme for the continuous, biocatalytic production of organosilicons.

## Introduction

Evolutionary engineered, biological systems frequently offer advantages over many conventional chemical processes, including higher chemo-, regio- and stereoselectivity in product formation, optimal activity under mild physiological conditions, and environmentally friendly production and work-up.<sup>[1]</sup> Recently the discovery and optimisation of biocatalysts with “new-to-nature” functions has opened up new classes of products for efficient biocatalytic processes.<sup>[2]</sup> In their ground-breaking work, Frances H. Arnold and her group demonstrated how the metalloporphyrin centre in engineered cytochrome enzymes can be used to catalyse production of highly reactive metal carbenes from diazo compounds, thereby realizing completely novel synthetic routes employing enzymes tailored via directed evolution.<sup>[3]</sup> Depending on the substrate and protein,<sup>[4]</sup> a variety of reactions are feasible,<sup>[5]</sup> including the highly specific and effective formation of silicon-carbon bonds<sup>[6]</sup> by cytochrome c variants from *Rhodothermus marinus*.<sup>[7]</sup> Directed evolution led to the triple mutant enzyme CytC(TDE), which achieved a 15-fold higher turnover number (TON) than comparable synthetic routes for this reaction type, with high stereoselectivity under anaerobic and reductive conditions. However, to improve the

efficacy of the reaction, it would be desirable to allow reusability of the catalyst and prolonged reaction times, which increase the TON and thus efficient use of these interesting biocatalysts.

Enzyme immobilisation, especially in combination with continuous flow operations, can address such issues and improve the biocatalytic process.<sup>[8]</sup>

The recovery of biocatalysts via heterogenisation, usually on a solid phase, is perfectly compatible with further chemical or biological strategies for enzyme optimisation.<sup>[9]</sup> This particularly applies to novel, flexible reactor concepts based on genetically encodable protein-based immobilisation tags.<sup>[8c,10]</sup> Especially the covalent SpyTag/ SpyCatcher (ST/SC) system, based on a rapidly formed isopeptide bond,<sup>[10g,11]</sup> offers precise control over the enzyme orientation, avoiding undirected catalyst immobilisation often accompanied by enzyme inactivation, while maintaining the benefits of a stable, covalent interaction between catalyst and support matrix.<sup>[12]</sup> Considering the elegant simplicity and efficiency of this versatile, self-assembling system, it already unlocked a variety of immobilisation strategies for biocatalysts<sup>[12b,13]</sup> and enabled the engineering of molecular systems in a wide range of applications.<sup>[14]</sup>

To further exploit the enormous application potential of the CytC(TDE) enzyme for the synthesis of high-value organosilicon compounds,<sup>[15]</sup> we report here a suitable immobilisation strategy using ST/SC chemistry (Figure 1), which enables the reuse of the enzyme as well as continuous biocatalytic synthesis in flow reactors in order to achieve a higher TON. For this purpose, we first genetically fused CytC(TDE) with a ST and investigated the influence of the peptide tag on its activity. We then immobilised the ST-modified enzyme on a particulate carrier material functionalised with the complementary SC-protein, and analysed the catalytic performance in batch as well as in a flow reactor format to facilitate the continuous synthesis of organosilicon **3** from ethyl 2-diazopropanoate **1** and phenyl dimethylsilane **2**.

[a] Dr. S. Gallus,<sup>+</sup> Dr. E. Mittmann,<sup>+</sup> A. J. Weber,<sup>+</sup> M. Peng, Prof. C. M. Niemeyer, Dr. K. S. Rabe  
 Institute for Biological Interfaces (IBG1)  
 Karlsruhe Institute of Technology (KIT)  
 Hermann-von-Helmholtz-Platz 1  
 76344 Eggenstein-Leopoldshafen (Germany)  
 E-mail: kersten.rabe@kit.edu

[\*] These authors contributed equally to this work

 Supporting information for this article is available on the WWW under <https://doi.org/10.1002/cctc.202300061>

 © 2023 The Authors. ChemCatChem published by Wiley-VCH GmbH. This is an open access article under the terms of the Creative Commons Attribution License, which permits use, distribution and reproduction in any medium, provided the original work is properly cited.

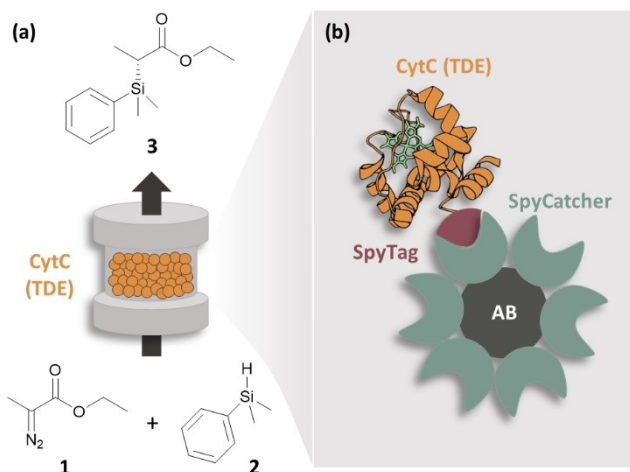


**Figure 1.** Flow biocatalysis for carbon-silicon bond formation. (a) The engineered biocatalyst CytC(TDE) was immobilised in a microfluidic packed-bed reactor to catalyse a reaction between ethyl 2-diazopropanoate **1** and phenyl dimethylsilane **2** to produce the organosilicon product **3**. (b) For immobilisation CytC(TDE) was genetically modified with a SpyTag (ST) and subsequently coupled to agarose beads (AB) bearing a complementary SpyCatcher (SC) unit.

## Results and Discussion

### Construction, generation and characterisation of ST-modified variants of CytC(TDE)

To enable efficient recycling of immobilised biocatalysts and to achieve high accumulated space-time-yields in flow biocatalysis covalent immobilisation strategies are desirable, as they provide an irreversible and stable interaction with the support matrix and therefore prevent catalyst leaching, which is commonly observed in methods using physical adsorption.<sup>[8b,16]</sup> To simultaneously maintain the advantages of a directed and specific protein immobilisation, we intended to use the self-assembled immobilisation technique provided by the ST/SC chemistry. To this end, we genetically fused the previously described CytC(TDE)<sup>[6]</sup> (CC) with a ST (Figure 2a). In the course of our studies we compared three ST variants which differed in the ST position as well as in the length of the linker sequence between the enzyme and the ST (Figure S1). Expression and purification revealed that a variant in which the ST is fused to its N-terminus via a single flexible GGGGS linker exhibited the best purity, expression yield and catalytic activity (ST-CC, Figure 2a, for detailed schematics of the genetic construction see Figure S1).

A comparison of purified CC and ST-CC via gelelectrophoretic analysis showed that CC (lacking the ST) appeared as a single band, while ST-CC showed two bands (Figure 2b). This effect may be due to the recently described cleavage of the ST by the native tail-specific protease (Tsp) in the periplasm of *E. coli*.<sup>[17]</sup> During expression, CytC(TDE) needs to be transferred to the periplasm for maturation, resulting in the proposed cleavage of the enzyme, which then exhibits a non-functional ST. Due to the reduced molecular mass, it was assumed that the lower band (Figure 2b, \*\*) in the SDS-PA-gel corresponds to the

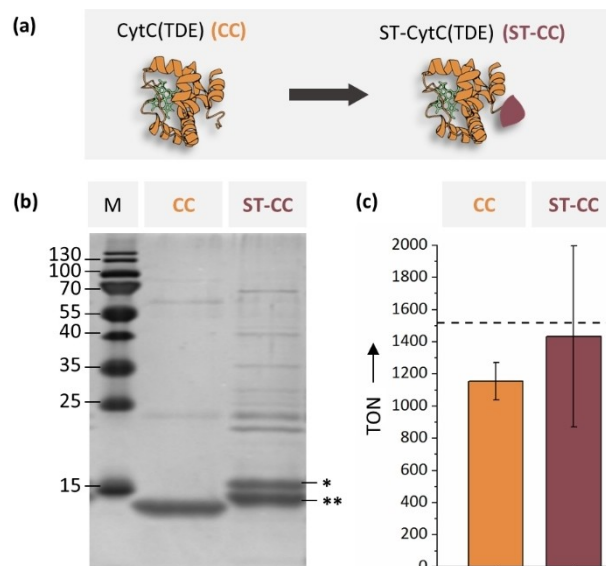


**Figure 2.** Modification of CytC(TDE) with the ST. (a) The previously described CytC(TDE) (CC) was genetically fused with a N-terminal ST to yield the fusion protein ST-CytC(TDE) (ST-CC). (b) Coomassie-stained SDS-PAGE of CC and ST-CC after purification via Ni<sup>2+</sup> affinity chromatography. The molecular weight of protein marker bands (M) is given in kDa. The unmodified CC appeared as a single band, while ST-CC appeared as two bands (\* and \*\*), the lower of which (\*\*) is presumably formed by partial cleavage of the ST by periplasmic proteases. (c) Catalytic activity as determined by incubation of 1  $\mu$ M enzyme with 10 mM substrate **1**, 10 mM substrate **2**, 10 mM Na<sub>2</sub>S<sub>2</sub>O<sub>8</sub>, 5% MeCN in M9-N buffer under anaerobic conditions for 4 h at room temperature. Activities are indicated as turn over numbers (TON), which are defined as the quotient of the amount of product formed during this reaction time and the amount of enzyme used. Note that TON refers to both cleaved and full-length protein. The dashed reference line indicates the previously reported total turnover number (TTN) for CC of 1518.<sup>[6]</sup> Error bars were obtained from at least two independent experiments.

truncated protein, while only the upper band (Figure 2b, \*) can be assigned to the complete protein with functional ST. This hypothesis was verified by using a time-resolved gelelectrophoretic analysis of the bond formation with a SC-modified coupling partner,<sup>[13b]</sup> where no covalent coupling to the SC-protein could be observed in case of the lower band, while the full-length protein in the upper band completely reacted to the desired SC-ST conjugate within 60 min (Figure S2). The full-length fusion protein thus contains a fully functional ST which can be utilised for immobilisation. In perspective, *E. coli* knock-out strains that prevent the expression of the protease Tsp<sup>[17]</sup> or the use of other bioconjugation systems such as the Snoop-Catcher/SnoopTag system<sup>[10f]</sup> could lead to improved yields of the full-length protein.

Using the model reaction for synthesis of the organosilicon compound **3** and a previously established GC analysis<sup>[6]</sup> (Figure S3), we found that ST-CC showed a similar TON after 4 h when compared to CC (Figure 2c). The TONs were both within the range of the reported total turnover number (TTN) for CC of 1518<sup>[6]</sup> (Figure 2c, dashed reference line), which represents the maximum TON that could be obtained before the reaction ultimately stopped within a reaction time of 1.5 h at room

temperature (RT). These results suggested that the additional ST on the protein has no distinct effect on the enzyme activity.

### ST-CC can be efficiently immobilised on agarose particles via ST/SC chemistry

To validate the suitability of ST-CC for immobilisation, we prepared SC-modified agarose beads (SC-AB) to which ST-CC was coupled to yield ST-CC@AB (Figure 3a). To benchmark the process, we determined the specific enzyme loading on the beads. Since it has been reported earlier that heme proteins such as ST-CC can be quantified fluorometrically,<sup>[18]</sup> we set up a fluorescence-based method which allows direct quantification of the covalently coupled ST-CC on AB. This method utilizes the fact that the heme group in the ST-CC contains a porphyrin that exhibits specific absorption at wavelengths in the range of 400 nm (Soret band). Removing the iron ion with high concentrations of boiling oxalic acid (OA) results in demetalised, free-base porphyrins, which exhibit a fluorescence at around 600 nm when excited at 400 nm (Figure 3b).<sup>[18]</sup>

We first used free ST-CC to validate the applicability of the method. To this end, ST-CC was boiled in 1 M oxalic acid for 30 min at 99 °C. Subsequently, we recorded an absorption spectrum and identified the absorption maximum at a wavelength of  $\lambda_{\text{ex}}=400$  nm (Figure 3c). Upon excitation at this wavelength, a fluorescence emission spectrum was obtained exhibiting a fluorescence maximum at a wavelength of  $\lambda_{\text{em}}=600$  nm (Figure 3d). Although untreated ST-CC similarly exhibited the Soret band, no fluorescence could be observed at  $\lambda_{\text{em}}=$

600 nm. To calculate the amount of immobilized enzyme, samples of ST-CC@AB were recorded along with a calibration curve using free ST-CC in a range of 5 to 50 pmol (Figure 3e). Using this method for two individual ST-CC@AB samples, we determined an average enzyme amount of  $23 \pm 4$  pmol<sub>ST-CC</sub>, which corresponds to an average amount of immobilised ST-CC of  $93 \pm 16$  pmol<sub>ST-CC</sub> per  $\mu\text{L}_{\text{AB}}$  carrier material.

### Optimising reaction conditions for the reuse of immobilised ST-CC and its application in continuous reactions

The quantification of immobilised ST-CC on the carrier material enabled us to compare its enzymatic activity to that of the free enzyme. In the course of these experiments, we observed yields of 3 well below 100%, while only small amounts of 1 were detectable in the reaction solution (data not shown). Diazo compounds are a highly reactive class of substances that can undergo  $\alpha$ -substitutions under release of molecular nitrogen. Thus, the full conversion of the diazo ester substrate 1 to the organosilicon 3 might be hampered by the limited stability of the highly reactive substrate 1 in aqueous solutions. In fact, we observed typical decomposition behaviour under anaerobic conditions in the M9-N reaction buffer, which is commonly used for these reactions (Figure 4a, b). While substrate 1 was stable in 100% MeCN, it quickly decomposed in a 5% MeCN in M9-N mixture. In 25% MeCN, the decomposition was less pronounced, so that after 360 min about 20% of the starting material was still present. We therefore investigated the effect of 5%, 25% and 50% of the co-solvent MeCN on the activity of

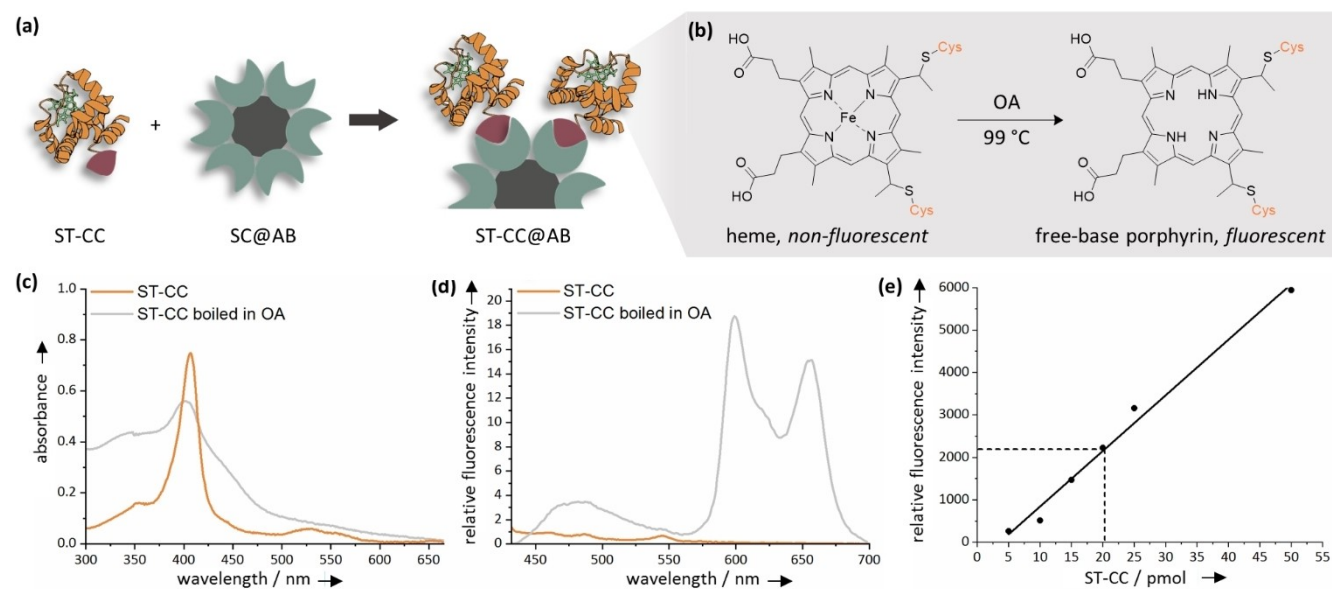


**Figure 3.** Quantification of the immobilisation of ST-CC on agarose beads. (a) ST-CC was incubated with agarose beads (AB) bearing a SC binding unit, thus leading to covalent attachment through the specific ST/SC interaction. (b) To quantify the amount of immobilised ST-CC, the beads were boiled in oxalic acid (OA) at 99 °C, leading to removal of the central iron atom of the heme cofactor,<sup>[18]</sup> thereby producing fluorescent free-base porphyrin which was quantified via fluorescence measurements. (c, d) Absorption and fluorescence spectra of ST-CC before (orange) and after (grey) boiling in OA. (e) Exemplary experimental data set for the quantification of ST-CC on AB. Samples were measured with  $\lambda_{\text{ex}}=400$  nm and  $\lambda_{\text{em}}=600$  nm after boiling in OA. Measurements of defined quantities of free ST-CC (dots) were used to calculate a linear calibration curve (solid line). The calibration was then used to determine the amount of immobilised ST-CC in a simultaneously measured ST-CC@AB sample based on its fluorescence value (dashed lines).

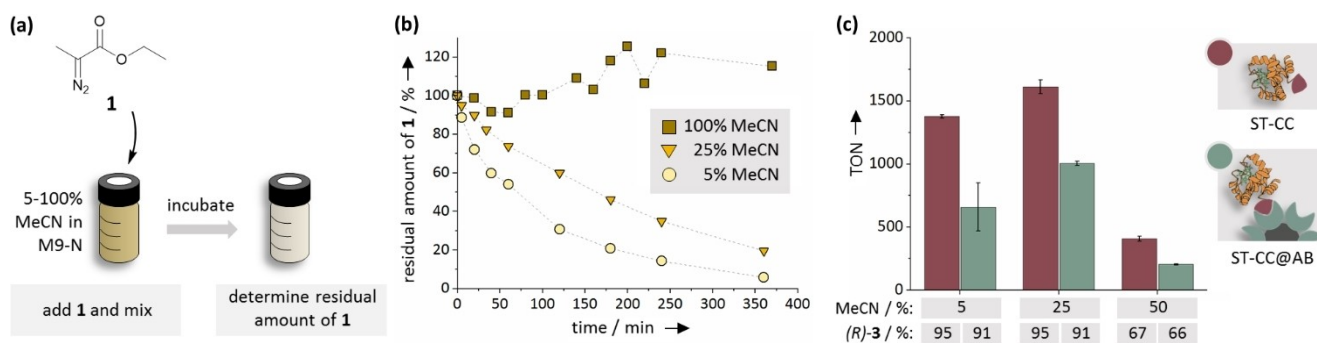


**Figure 4.** Impact of the fraction of co-solvent MeCN on the stability and enzymatic conversion of substrate **1**. (a) 10 mM of substrate **1** were added to 5% or 25% MeCN in M9-N, containing 10 mM  $\text{Na}_2\text{S}_2\text{O}_4$ , or to 100% MeCN. The mixtures were incubated for 360 min at room temperature under anaerobic conditions. (b) At defined time points the residual amount of substrate **1** was determined by GC analysis. (c) Impact of the fraction of the co-solvent MeCN on the TON of ST-CC (red) or ST-CC@AB (green) as determined by GC analysis. Reactions were performed using 1.4 nmol of ST-CC or 15  $\mu\text{L}$  ST-CC@AB (corresponding to approx. 1.4 nmol immobilised ST-CC), 10 mM substrate **1**, 10 mM substrate **2**, 10 mM  $\text{Na}_2\text{S}_2\text{O}_4$ , 5–50% MeCN in M9-N at room temperature under anaerobic conditions for 4 h. Error bars were obtained from two independent experiments. The proportion of (*R*)-configured organosilicon product **3** was determined by chiral HPLC analysis.

free and immobilised ST-CC (Figure 4c). Both the free as well as the immobilised ST-CC showed the highest TON in 25% MeCN, while maintaining a high stereospecificity, as has been reported before in case of other carbene transferases.<sup>[19]</sup> This could be due to either higher enzyme activity or lower decomposition of substrate **1** under these reaction conditions, resulting in higher substrate availability. Since the use of 25% MeCN as co-solvent resulted in increased product formation either way, this condition was used in all subsequent reactions. Under these conditions, the immobilised enzyme showed a reduced enzymatic activity of approx. 60% compared to the free enzyme.

We then investigated, whether the yield of the reaction can also be limited by the availability of silane **2**. As expected, we did not observe significant decomposition, however, we actually found that only a portion of the silane was dissolved in 25% MeCN in M9-N at room temperature. Indeed, experiments indicated that concentrations higher than 5 mM could not be recovered from the reaction buffer because a two-phase system with insoluble droplets of **2** occurred at these higher concentrations (Figure S4). To avoid this two-phase system and to enable proper mixing in all further experiments, we chose to switch to a lower concentration of 2.5 mM of substrate **2**, in which the silane is dissolved and available for the enzymatic conversion.

We assumed that potential losses in yield due to the limited stability of substrate **1** under these reaction conditions could be reduced either by repeatedly preparing a fresh reaction mixture of substrate **1** from a 100% MeCN stock solution using a sequential batch approach, or else by employing a continuously operated packed-bed reactor into which substrate **1** is supplied as a solution in pure MeCN. To this end, we first established a syringe pump operated setup in an anaerobic chamber feeding a home-made PTFE packed bed reactor<sup>[10d]</sup> filled with 100  $\mu\text{L}$  ST-CC@AB (Figure 5a, b). During the initial tests, we found that precipitation occurred when M9-N was mixed with MeCN in a T-junction mixer structure. However, this effect could be avoided using  $\text{NaP}_i$  (50 mM sodium phosphates, pH 7.4) con-

taining fewer salts (Figure S5). We also constructed the entire flow-path out of either glass or PTFE parts, as we observed strong adsorption of **2** to silicone materials. Combining all optimisations, we used two syringes in parallel, one containing the substrates **1** and **2** in pure MeCN at a flow rate of 2.5  $\mu\text{L}\cdot\text{min}^{-1}$ , while a second syringe contained the reducing agent  $\text{Na}_2\text{S}_2\text{O}_4$  in  $\text{NaP}_i$  at a flow rate of 7.5  $\mu\text{L}\cdot\text{min}^{-1}$ . The solutions were pumped separately into the continuous flow system and mixed shortly before the reactor using the glass T-junction chip.

This procedure allowed us to minimise the preincubation time of the substrates with the aqueous buffer, while at the same time ensured the optimal solvent concentration of 25% MeCN at the combined flow rate of 10  $\mu\text{L}\cdot\text{min}^{-1}$  resulting in a residence time of 2.6 min. Quantitative GC analysis of the effluent showed that after the void volume of the setup was filled with reactants (approx. 40 min), the reactor produced the desired product **3** with only small amounts of substrates **1** and **2** remaining (Figure 5c). Long-term experiments revealed that the product formation remained stable for at least 4 days (Figure S6).

After the entire effluent collected over this period was extracted in cyclohexane and the solvent was removed under reduced pressure, the identity of the desired product **3** could also be clearly confirmed by  $^1\text{H}$  NMR (Figure S7). Under these conditions, substrates **1** and **2** were no longer detectable, as they were easily removed by evaporation under reduced pressure. By means of this simple work-up, **3** could be recovered in good purity directly from the reactor.

To expand the range of applications for our immobilised enzyme, we also applied ST-CC@AB in sequential batch experiments, in which the reaction solution was exchanged daily to provide fresh substrates resulting in a process time of 1 day. Again, we found stable production of **3** over at least 4 days (Figure S8), demonstrating the good recyclability of ST-CC@AB. To evaluate the performance of the packed-bed and sequential batch formats and to compare them with conventional batch

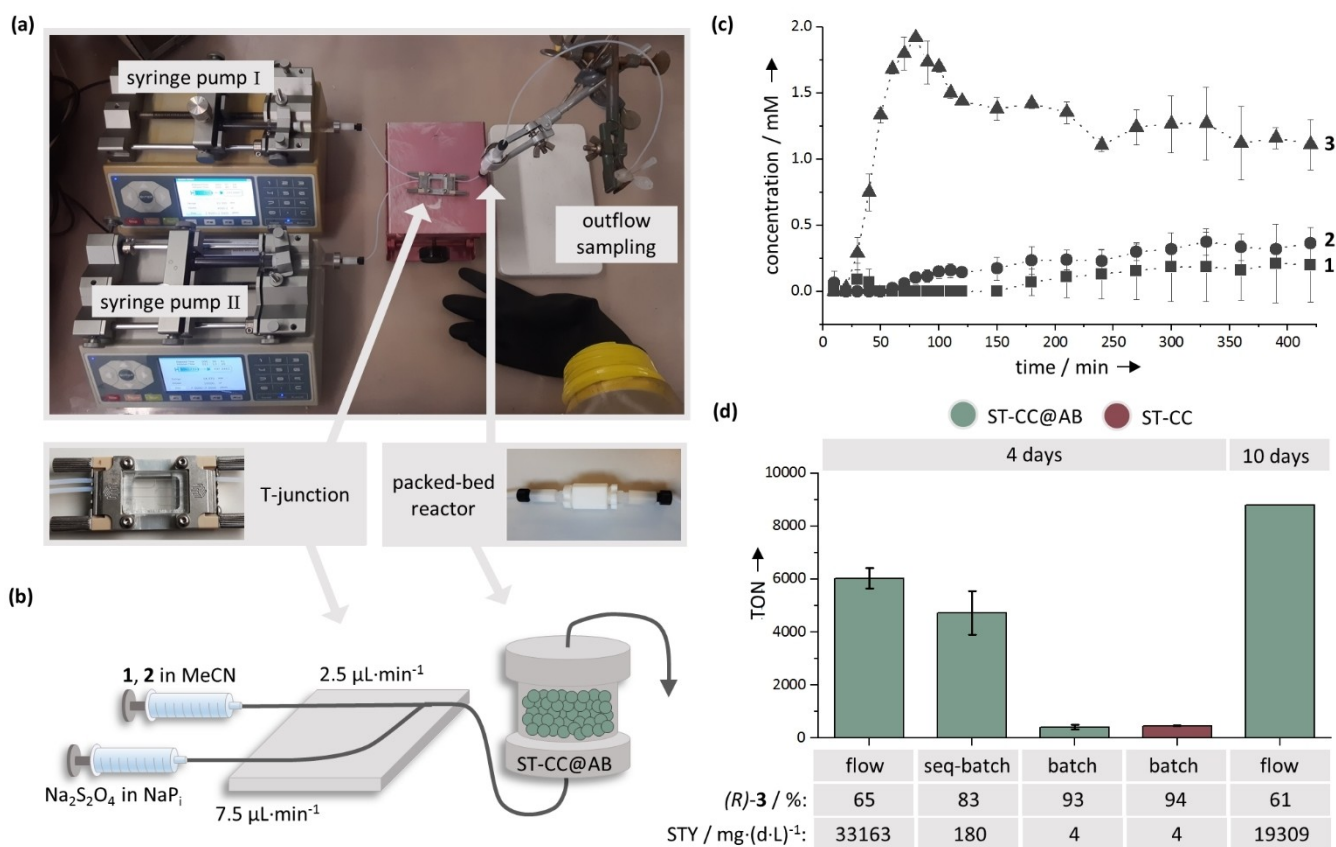


**Figure 5.** Biocatalytic production of **3** using immobilised ST-CC in flow and in batch. (a) Microfluidic setup in an anaerobic chamber. Two syringe pumps facilitate flow of buffer and substrate solutions, which are conjoined by a T-junction to enter a packed-bed reactor filled with ST-CC@AB. (b) Syringe I was filled with 10 mM of substrates **1** and **2** in MeCN, syringe II with 13.3 mM of Na<sub>2</sub>S<sub>2</sub>O<sub>4</sub> in NaP<sub>i</sub>. Using flow rates of 2.5 μL·min<sup>-1</sup> and 7.5 μL·min<sup>-1</sup> respectively, the following conditions were achieved in the reactor: 2.5 mM **1**, 2.5 mM **2**, 10 mM Na<sub>2</sub>S<sub>2</sub>O<sub>4</sub>, 25% MeCN in NaP<sub>i</sub> at room temperature with a total flow rate of 10 μL·min<sup>-1</sup> with a residence time of 2.6 min. (c) Concentration of substrates **1**, **2** and product **3** in the outflow of the packed-bed reactor quantified by GC analysis. (d) TON of ST-CC@AB in the packed-bed reactor (flow) as well as a sequential batch format (seq-batch) after a total period of 4 days compared to conventional batch experiments (batch) using ST-CC@AB (green) or free ST-CC (red) under identical conditions. All experiments were performed using the same total amount of ST-CC (9.3 nmol) and 2.5 mM of substrates **1** and **2**. Error bars were obtained from two independent experiments. The corresponding space time yields (STY) were calculated and the proportion of (*R*)-configured organosilicon product **3** was determined by chiral HPLC analysis. The residence time of the flow reactions is only 2.6 min, whereas in the batch experiments is 4 days and in the sequential batch 1 day.

experiments in which ST-CC@AB or free ST-CC were incubated continuously in the same reaction solution, we calculated the TON and space time yields (STY) for all approaches over a total period of 4 days (Figure 5d). As expected, both the continuous and sequential batch methods yielded much higher TONs, and thus much higher STYs, than the batch experiments, where the competitive decomposition of substrate **1** in aqueous solutions resulted in comparatively low TONs. Thus, the immobilisation of ST-CC on beads combined with the continuous or repetitive replacement of the substrate solution allowed for substantially increased productivity of the enzyme. ST-CC@AB remained active within the flow reactor after the fourth day and even after extending the operational time of the reactor to 10 days, which increased the TON even further to about 9000 (Figure 5d).

However, when using the flow or sequential batch approaches, reduced stereoselectivities were observed compared to the batch experiments. This indicates that the correct folding of the enzyme might be impaired when the enzyme

remains in high concentrations of 25% MeCN for a long time, thus negatively affecting the stereoselectivity. In batch systems, **3** is only produced for a comparatively short time due to the rapid decomposition of **1**. In this case, partial unfolding of the enzyme, which would lead to a loss of stereoselectivity, would not be observed. However, under reaction conditions where the substrate is repeatedly supplied, the partially unfolded enzyme would be able to convert the substrate, resulting in lower stereoselectivity. Future studies could elucidate the effects of varying concentrations of MeCN as a co-solvent, but this would require the development of a flow reaction setup that would allow the syringe pumps to be operated under significantly different flow rates. An alternative explanation could be the modification of the enzyme itself. For a similar heme-containing biocatalyst, Renata *et al.* reported the reaction of the *in situ* formed carbene to amino acids in the vicinity of the active centre.<sup>[20]</sup> Such a mechanism could also take effect here and impair the stereoselectivity of the enzyme. Since fresh substrate **1** is constantly being supplied in the flow and sequential batch

experiments, the effect might be more pronounced than in the batch experiments, where substrate **1** decomposes quickly. As previously demonstrated, this issue might be avoided by identifying and replacing the relevant amino acids in the active centre.<sup>[20]</sup>

## Conclusion

In summary, we demonstrate here that the enzyme CytC(TDE) can be immobilised efficiently via the self-assembling ST/SC system. We developed analytical methods to quantify and directly compare TONs for the free and immobilised enzyme and we could show that the immobilised biocatalyst can be employed in sequential batch reactions as well as in continuous flow reaction processes to produce organosilicons with improved TONs. We were further able to establish a flow reactor setup with inline mixing under anaerobic conditions and via the optimisation of the reaction conditions as well as the immobilisation of CytC(TDE) we were able to get a better insight into factors limiting the TON and modulating the stereoselectivity of this interesting biocatalyst. Although we already achieved a 6-fold increase in TON in comparison to earlier reports, optimisation of the enzyme, the reaction conditions as well as the flow setup might enable further improvements towards a more economically feasible application of this and similar heme-containing enzymes.

## Experimental Section

Experimental details on the synthesis of substrate **1**, the construction of plasmids, the analysis of proteins as well as on the performance of GC and HPLC analysis are given in the Supporting Information.

### Protein expression and purification

PAD-SC-His<sup>[13b]</sup> and His-SC<sup>[13c]</sup> were produced as described previously. For the production of CC variants, the respective expression plasmid was co-transformed with the cytochrome c maturation plasmid pEC86<sup>[21]</sup> (Culture Collection of Switzerland, plasmid no. CCOS 891) into *E. coli* BL21(DE3) using electroporation. *E. coli* cells harbouring both plasmids were selected overnight on LB/agar plates containing 30  $\mu\text{g mL}^{-1}$  chloramphenicol and 100  $\mu\text{g mL}^{-1}$  ampicillin at 37 °C. 200 mL of LB<sup>chl+Amp</sup> were inoculated with a single colony and incubated overnight at 37 °C and 180 rpm. Four flasks with 2 L LB<sup>chl+Amp</sup> were inoculated with 40 mL of this overnight culture and incubated at 37 °C and 180 rpm until an OD<sub>600</sub> of 0.6 was reached. The culture was then cooled on ice for 20 min and induced by adding 20  $\mu\text{M}$  isopropyl  $\beta$ -D-1-thiogalactopyranoside (IPTG) and 200  $\mu\text{M}$  5-aminolevulinic acid. After incubation at 20 °C and 180 rpm for 20 h cells were harvested by centrifugation (10,000 rcf, 4 °C, 10 min), resuspended in 40 mL NP<sub>10</sub> buffer (500 mM NaCl, 50 mM NaH<sub>2</sub>PO<sub>4</sub>, 10 mM imidazole, pH 8.0) and stored at -80 °C until further processing. The cell suspension was thawed at 25 °C in a water bath and subsequently incubated with DNaseI and lysozyme (AppliChem) for 30 min at room temperature. After further cell disruption using ultrasonication, cell debris was removed using centrifugation (45,000 rcf, 4 °C, 1 h) and the protein rich supernatant filtered through a 0.45  $\mu\text{m}$

Durapore PVDF membrane (Steriflip, Millipore). Purification was performed using an FPLC (fast protein liquid chromatography) system (Äkta pure, GE Healthcare) equipped with a nickel iminodiacetate (Ni-IDA) cartridge (1 mL or 5 mL HisTrap FF, GE Healthcare). After applying the lysate, the column was washed with a mixture of 2% NP<sub>10</sub> (500 mM NaCl, 50 mM NaH<sub>2</sub>PO<sub>4</sub>, 500 mM Imidazol, pH 8.0) and 98% NP<sub>10</sub>. Subsequently the protein was eluted using a linear gradient (2% to 100% NP<sub>10</sub>) over 10 column volumes. The collected fractions containing the purified protein were combined and the buffer exchanged to NaP<sub>i</sub> (25 mM sodium phosphate, pH 7.4) using Vivaspin 20, 5,000 MWCO concentrators (Sartorius).

### Protein immobilization

Agarose epoxy beads (AB, PureCube Epoxy Activated Agarose, Cube Biotech) were functionalised with SC proteins via its amino groups as previously reported<sup>[10a]</sup> following the manufacturer's instructions. The resulting SC-AB were then incubated with 500 pmol ST-CC per  $\mu\text{L}$  of SC-AB in NaP<sub>i</sub> for 1 h at 30 °C and 1,000 rpm. The beads with immobilised enzyme (ST-CC@AB) were subsequently washed five times with NaP<sub>i</sub>.

### Quantification of immobilised protein via heme-based fluorescence assay

A solution of 2 M oxalic acid (OA) was freshly prepared by heating to 65 °C to completely dissolve the OA. **Recording of UV-Vis and fluorescence spectra.** 80  $\mu\text{L}$  of a 90  $\mu\text{M}$  solution of ST-CC in NaP<sub>i</sub> was mixed with 80  $\mu\text{L}$  of the OA solution, incubated at 99 °C for 30 min and diluted appropriately in NaP<sub>i</sub> to record the spectra in a glass cuvette with a pathlength of 1 cm. UV-Vis spectra were recorded using a final concentration of 15  $\mu\text{M}$  ST-CC boiled in OA or 5  $\mu\text{M}$  of untreated ST-CC. Fluorescence spectra were recorded using a final concentration of 30  $\mu\text{M}$  boiled or untreated ST-CC with an excitation wavelength of  $\lambda_{\text{ex}} = 400$  nm. **Quantification of ST-CC@AB.** 0.33  $\mu\text{L}$  of ST-CC@AB in 80  $\mu\text{L}$  of NaP<sub>i</sub> were mixed with 80  $\mu\text{L}$  of the OA solution and incubated at 99 °C for 30 min. Samples were centrifuged and 120  $\mu\text{L}$  of the supernatant were transferred to a 96-well microtiter plate (Nunc™ F96 MicroWell™ Black Polystyrene Plate, non-treated surface, Thermo Scientific). The fluorescence of the free-base porphyrin was recorded in a microplate reader (Synergy H1 Hybrid Reader, BioTek) at 30 °C using an excitation wavelength of  $\lambda_{\text{ex}} = 400$  nm and an emission wavelength of  $\lambda_{\text{em}} = 600$  nm. Please note that a strong influence of the sample treatment on the fluorescence intensity in this very sensitive method was observed.<sup>[18]</sup> To minimise this influence, each ST-CC@AB sample was recorded along with a separate calibration curve using free ST-CC in a range of 5 to 50 pmol. The calibration samples were treated and measured according to the procedure described above.

### Analytical scale enzymatic reactions

The activity of soluble or immobilised CC variants was studied in an anaerobic vinyl chamber using an adapted protocol of Kan *et al.*<sup>[6]</sup> In a total volume of 400  $\mu\text{L}$  of anaerobic M9-N buffer (47.7 mM Na<sub>2</sub>HPO<sub>4</sub>, 22 mM KH<sub>2</sub>PO<sub>4</sub>, 8.6 mM NaCl, 2 mM MgSO<sub>4</sub>, 0.1 mM CaCl<sub>2</sub>, pH 7.4) containing varying amounts of MeCN (5%, 25%, or 50%), 1–3.5  $\mu\text{M}$  of soluble CC variants or 15  $\mu\text{L}$  ST-CC@AB were mixed with 10 mM Na<sub>2</sub>S<sub>2</sub>O<sub>4</sub>, 10 mM ethyl 2-diazopropanoate (**1**) and 10 mM phenyl dimethylsilane (**2**). The components were mixed in a 1.5 mL crimp vial and incubated anaerobically at 700 rpm and 25 °C for 4 h on a "MKR13 (Hettich Benelux)" shaker. The reaction was stopped by adding cyclohexane and analysed by GC or chiral HPLC.

Turnover numbers (TONs) were calculated from the quotient of the amount of product formed within the specified reaction time and the amount of enzyme used (Eq. 1):

$$\text{TON} = n_{\text{product}}/n_{\text{enzyme}} \quad (1)$$

### Scale-up of enzymatic reactions

**Continuous flow reactions.** The complete microfluidic setup was placed and operated inside an anaerobic vinyl chamber. All modules were connected with PTFE tubing (ID 0.5 mm). A custom-made PTFE-reactor,<sup>[10d]</sup> fabricated by the Institute of Astroparticle Physics at the Karlsruhe Institute of Technology, was loaded with 100  $\mu\text{L}$  ST-CC@AB and closed with filter paper to retain the immobilised biocatalyst (Qualitative filter paper, 143, particle retention: 5–13  $\mu\text{m}$ , VWR). Glass syringes (5 or 10 mL, 1005 C SYR,  $1/4$ -28 threads, Hamilton) were mounted in two separate syringe pumps (Nexus 3000 Push Pull, Chemyx). One syringe was filled with the substrate solution consisting of 10 mM each of 1 and 2 in pure MeCN and operated at a flow rate of  $2.5 \mu\text{L} \cdot \text{min}^{-1}$ , the second with a buffer solution consisting of 13.3 mM  $\text{Na}_2\text{S}_2\text{O}_4$  in anaerobic  $\text{NaP}_i$  and at  $7.5 \mu\text{L} \cdot \text{min}^{-1}$ . The solution streams were combined in a T-junction chip (Large Droplet Junction Chip, glass, 100  $\mu\text{m}$  channel width, hydrophilic, H Interface, Dolomite), resulting in a reaction solution containing 2.5 mM 1 and 2 and 10 mM  $\text{Na}_2\text{S}_2\text{O}_4$  in 25% MeCN in  $\text{NaP}_i$ , and a combined flow rate of  $10 \mu\text{L} \cdot \text{min}^{-1}$ , which was then connected to the reactor. The reactor effluent was manually fractionated and subsequently analysed by GC or chiral HPLC.

**Sequential batch reactions.** In a glass vial, 2.5 mM ethyl 2-diazopropanoate (1), 2.5 mM phenyl dimethylsilane (2), 10 mM  $\text{Na}_2\text{S}_2\text{O}_4$ , and 100  $\mu\text{L}$  ST-CC@AB were incubated in a total volume of 14.4 mL anaerobic  $\text{NaP}_i$  with 25% MeCN under continuous shaking at 700 rpm on a "TS-100 (Peglab)" shaker (resulting centrifugal force: 1 rcf). Every 24 h, the ST-CC@AB were sedimented, the supernatant was removed and the ST-CC@AB resuspended in a fresh reaction solution with the same composition. The supernatant was then analysed by GC or chiral HPLC. **Conventional one-pot batch reactions.** In glass bottles, 2.5 mM ethyl 2-diazopropanoate (1), 2.5 mM phenyl dimethylsilane (2), 10 mM  $\text{Na}_2\text{S}_2\text{O}_4$ , and 100  $\mu\text{L}$  ST-CC@AB or 9.3 nmol of soluble ST-CC were incubated in a total volume of 57.6 mL anaerobic  $\text{NaP}_i$  with 25% MeCN for four days under continuous shaking at 190 rpm on a "Multitron Pro (Infors HT)" shaker (resulting centrifugal force: 1 rcf). The supernatant was then analysed by GC or chiral HPLC. **Calculation of residence times and space time yields (STY).** For the calculation of the residence time, an estimation of the void volume or mean bed porosity is necessary. While the calculation of the mean bed porosity for a regular arrangement of equally sized ideal spheres can be derived by mathematical considerations, the mean porosity of randomly packed reactor beds is a complex issue that depends on a variety of parameters and material constants. In comparison to regular packing, where the mean bed porosity varies between 0.26 and 0.48 depending on the arrangement, random packing can take values between 0.36 (random close packing) and 0.44 (random loose packing) when unconfined.<sup>[22]</sup> Since the ratio of tube-to-particle diameter is  $> 100$  in the case of the reactor used in this study, wall effects were neglected and the closest sphere packing was assumed, with a void volume  $\epsilon$  of 26% of the total reactor volume of 100  $\mu\text{L}$ . The residence time  $t_r$  was then calculated with  $Q$  as the total volumetric flow rate of  $10 \mu\text{L}/\text{min}$  (Eq. 2):

$$t_r = \epsilon/Q \quad (2)$$

Calculations for STY were performed based on the amount of product formed  $m_{\text{product}}$ , the reaction time  $t_r$  (4 or 10 days) and the volume  $V_{rs}$  of the reactor for flow reactions (100  $\mu\text{L}$ ) or the reaction solution (14.4 mL for sequential batch reaction and 57.6 mL for one-pot batch reactions) using the following formula (Eq. 3):

$$\text{STY} = m_{\text{product}}/(t_r \cdot V_{rs}) \quad (3)$$

### Acknowledgements

This work was supported through the Helmholtz program "Materials Systems Engineering" under the topic "Adaptive and Biostructive Materials Systems". S.G. and A.J.W. are grateful for support by a Kekulé fellowship by Fonds der Chemischen Industrie (FCI). We thank the Institute for Astroparticle Physics (IAP) for manufacturing the PTFE microreactors, Sophia Kunz for experimental support and Dr. Christoph Bickmann for helpful discussions. Open Access funding enabled and organized by Projekt DEAL.

### Conflict of Interest

The authors declare no conflict of interest.

### Data Availability Statement

The data that support the findings of this study are available from the corresponding author upon reasonable request.

**Keywords:** flow biocatalysis · immobilisation · cytochromes · organosilicons · SpyCatcher/SpyTag

- [1] a) E. L. Bell, W. Finnigan, S. P. France, A. P. Green, M. A. Hayes, L. J. Hepworth, S. L. Lovelock, H. Niikura, S. Osuna, E. Romero, K. S. Ryan, N. J. Turner, S. L. Flitsch, *Nat. Rev. Methods Primers* **2021**, *1*, 46; b) R. A. Sheldon, J. M. Woodley, *Chem. Rev.* **2018**, *118*, 801–838; c) R. A. A. Sheldon, D. Brady, M. L. L. Bode, *Chem. Sci.* **2020**, *11*, 2587–2605; d) S. K. Wu, R. Snajdrova, J. C. Moore, K. Baldenius, U. T. Bornscheuer, *Angew. Chem. Int. Ed.* **2021**, *60*, 88–119; *Angew. Chem.* **2021**, *133*, 89–123.
- [2] a) H. Renata, Z. J. Wang, F. H. Arnold, *Angew. Chem. Int. Ed.* **2015**, *54*, 3351–3367; *Angew. Chem.* **2015**, *127*, 3408–3426; b) K. Chen, F. H. Arnold, *Nat. Catal.* **2020**, *3*, 203–213; c) D. C. Miller, S. V. Athavale, F. H. Arnold, *Nat. Synth.* **2022**, *1*, 18–23; d) Q. Zhou, M. Chin, Y. Fu, P. Liu, Y. Yang, *Science* **2021**, *374*, 1612–1616; e) T. Vornholt, F. Christoffel, M. M. Pellizzoni, S. Panke, T. R. Ward, M. Jeschek, *Sci. Adv.* **2021**, *7*, eabe4208; f) T. Vornholt, M. Jeschek, *ChemBioChem* **2020**, *21*, 2241–2249; g) B. Hauer, *ACS Catal.* **2020**, *10*, 8418–8427.
- [3] R. D. Lewis, M. Garcia-Borràs, M. J. Chalkley, A. R. Buller, K. N. Houk, S. B. J. Kan, F. H. Arnold, *Proc. Natl. Acad. Sci. USA* **2018**, *115*, 7308–7313.
- [4] M. Garcia-Borràs, S. B. J. Kan, R. D. Lewis, A. Tang, G. Jimenez-Osés, F. H. Arnold, K. N. Houk, *J. Am. Chem. Soc.* **2021**, *143*, 7114–7123.
- [5] a) S. B. J. Kan, X. Huang, Y. Gumulya, K. Chen, F. H. Arnold, *Nature* **2017**, *552*, 132–136; b) X. Huang, M. Garcia-Borràs, K. Miao, S. B. J. Kan, A. Zutshi, K. N. Houk, F. H. Arnold, *ACS Cent. Sci.* **2019**, *5*, 270–276; c) P. S. Coelho, E. M. Brustad, A. Kannan, F. H. Arnold, *Science* **2013**, *339*, 307–310; d) Z. J. Wang, N. E. Peck, H. Renata, F. H. Arnold, *Chem. Sci.* **2014**, *5*, 598–601; e) K. Chen, X. Huang, S.-Q. Zhang, A. Z. Zhou, S. B. J. Kan, X. Hong, F. H. Arnold, *Synlett* **2019**, *30*, 378–382.
- [6] S. B. Kan, R. D. Lewis, K. Chen, F. H. Arnold, *Science* **2016**, *354*, 1048–1051.

- [7] M. Stelter, A. M. P. Melo, M. M. Pereira, C. M. Gomes, G. O. Hreggvidsson, S. Hjorleifsdottir, L. M. Saraiva, M. Teixeira, M. Archer, *Biochemistry* **2008**, *47*, 11953–11963.
- [8] a) Y. J. Zhu, Q. M. Chen, L. Y. Shao, Y. W. Jia, X. M. Zhang, *React. Chem. Eng.* **2020**, *5*, 9–32; b) P. Žnidaršič-Plazl, *Curr. Opin. Green Sustain. Chem.* **2021**, *32*, 100546; c) K. S. Rabe, J. Muller, M. Skoupi, C. M. Niemeyer, *Angew. Chem. Int. Ed.* **2017**, *56*, 13574–13589; *Angew. Chem.* **2017**, *129*, 13760–13777.
- [9] a) M. A. Huffman, A. Fryszkowska, O. Alvizo, M. Borra-Garske, K. R. Campos, K. A. Canada, P. N. Devine, D. Duan, J. H. Forstater, S. T. Grosser, H. M. Halsey, G. J. Hughes, J. Jo, L. A. Joyce, J. N. Kolev, J. Liang, K. M. Maloney, B. F. Mann, N. M. Marshall, M. McLaughlin, J. C. Moore, G. S. Murphy, C. C. Nawrat, J. Nazor, S. Novick, N. R. Patel, A. Rodriguez-Granillo, S. A. Robaire, E. C. Sherer, M. D. Truppo, A. M. Whittaker, D. Verma, L. Xiao, Y. Xu, H. Yang, *Science* **2019**, *366*, 1255–1259; b) R. C. Rodrigues, Á. Berenguer-Murcia, R. Fernandez-Lafuente, *Adv. Synth. Catal.* **2011**, *353*, 2216–2238.
- [10] a) T. Peschke, P. Bitterwolf, S. Hansen, J. Gasmi, K. S. Rabe, C. M. Niemeyer, *Catalysts* **2019**, *9*, 164; b) T. Peschke, P. Bitterwolf, K. S. Rabe, C. M. Niemeyer, *Chem. Eng. Technol.* **2019**, *42*, 2009–2017; c) J. Döbber, T. Gerlach, H. Offermann, D. Rother, M. Pohl, *Green Chem.* **2018**, *20*, 544–552; d) M. Peng, D. L. Siebert, M. K. M. Engqvist, C. M. Niemeyer, K. S. Rabe, *ChemBioChem* **2021**, *23*, e202100468; e) K. J. Koßmann, C. Ziegler, A. Angelin, R. Meyer, M. Skoupi, K. S. Rabe, C. M. Niemeyer, *ChemBioChem* **2016**, *17*, 1102–1106; f) G. Veggiani, T. Nakamura, M. D. Brenner, R. V. Gayet, J. Yan, C. V. Robinson, M. Howarth, *Proc. Natl. Acad. Sci. USA* **2016**, *113*, 1202–1207; g) B. Zakeri, J. O. Fierer, E. Celik, E. C. Chittock, U. Schwarz-Linek, V. T. Moy, M. Howarth, *Proc. Natl. Acad. Sci. USA* **2012**, *109*, E690–E697; h) S. Kröll, K. S. Rabe, C. M. Niemeyer, *Small* **2021**, *17*, 2105095; i) Y. Liu, D. Liu, W. Yang, X.-L. Wu, L. Lai, W.-B. Zhang, *Chem. Sci.* **2017**, *8*, 6577–6582; j) I. N. A. Khairil Anuar, A. Banerjee, A. H. Keeble, A. Carella, G. I. Nikov, M. Howarth, *Nat. Commun.* **2019**, *10*, 1734; k) E. J. Hartzell, J. Terr, W. Chen, *J. Am. Chem. Soc.* **2021**, *143*, 8572–8577.
- [11] a) A. H. Keeble, M. Howarth, *Chem. Sci.* **2020**, *11*, 7281–7291; b) J. O. Fierer, G. Veggiani, M. Howarth, *Proc. Natl. Acad. Sci. USA* **2014**, *111*, E1176–E1181; c) A. H. Keeble, P. Turkki, S. Stokes, I. N. A. Khairil Anuar, R. Rahikainen, V. P. Hytönen, M. Howarth, *Proc. Natl. Acad. Sci. USA* **2019**, *116*, 26523–26533.
- [12] a) G. P. Anderson, J. L. Liu, L. C. Shriver-Lake, D. Zabetakis, V. A. Sugiharto, H.-W. Chen, C.-R. Lee, G. N. Defang, S.-J. L. Wu, N. Venkateswaran, E. R. Goldman, *Anal. Chem.* **2019**, *91*, 9424–9429; b) G. Zhang, M. B. Quin, C. Schmidt-Dannert, *ACS Catal.* **2018**, *8*, 5611–5620; c) L. Cai, Y. Chu, X. Liu, Y. Qiu, Z. Ge, G. Zhang, *Microb. Cell Fact.* **2021**, *20*, 37; d) T. Burgahn, R. Garrecht, K. S. Rabe, C. M. Niemeyer, *Chem. Eur. J.* **2019**, *25*, 3483–3488.
- [13] a) T. Peschke, P. Bitterwolf, S. Gallus, Y. Hu, C. Oelschlaeger, N. Willenbacher, K. S. Rabe, C. M. Niemeyer, *Angew. Chem. Int. Ed.* **2018**, *57*, 17028–17032; *Angew. Chem.* **2018**, *130*, 17274–17278; b) E. Mittmann, S. Gallus, P. Bitterwolf, C. Oelschlaeger, N. Willenbacher, C. M. Niemeyer, K. S. Rabe, *Micromachines* **2019**, *10*; c) T. Peschke, K. S. Rabe, C. M. Niemeyer, *Angew. Chem. Int. Ed.* **2017**, *56*, 2183–2186; *Angew. Chem.* **2017**, *129*, 2215–2219; d) E. Mittmann, F. Mickoleit, D. S. Maier, S. Y. Stäbler, M. A. Klein, C. M. Niemeyer, K. S. Rabe, D. Schüler, *ACS Appl. Mater. Interfaces* **2022**, *14*, 22138–22150.
- [14] a) S. Thrane, C. M. Janitzek, S. Matondo, M. Resende, T. Gustavsson, W. A. de Jongh, S. Clemmensen, W. Roeffen, M. van de Vegte-Bolmer, G. J. van Gemert, R. Sauerwein, J. T. Schiller, M. A. Nielsen, T. G. Theander, A. Salanti, A. F. Sander, *J. Nanobiotechnol.* **2016**, *14*, 30; b) M. K. Alam, A. El-Sayed, K. Barreto, W. Bernhard, H. Fonge, C. R. Geyer, *Mol. Imaging Biol.* **2019**, *21*, 54–66; c) W. Ma, A. Saccardo, D. Roccatano, D. Aboagye-Mensah, M. Alkaseem, M. Jewkes, F. Di Nezza, M. Baron, M. Soloviev, E. Ferrari, *Nat. Commun.* **2018**, *9*, 1489; d) X. Ke, Y. Zhang, F. Zheng, Y. Liu, Z. Zheng, Y. Xu, H. Wang, *Chem. Commun.* **2018**, *54*, 1189–1192; e) M. K. Alam, C. Gonzalez, W. Hill, A. El-Sayed, H. Fonge, K. Barreto, C. R. Geyer, *ChemBioChem* **2017**, *18*, 2217–2221; f) J. Bao, N. Liu, L. Zhu, Q. Xu, H. Huang, L. Jiang, *J. Agric. Food Chem.* **2018**, *66*, 8061–8068; g) K. D. Brune, D. B. Leneghan, I. J. Brian, A. S. Ishizuka, M. F. Bachmann, S. J. Draper, S. Biswas, M. Howarth, *Sci. Rep.* **2016**, *6*, 19234; h) L. Jia, K. Minamihata, H. Ichinose, K. Tsumoto, N. Kamiya, *Biotechnol. J.* **2017**, *12*; i) S. Thrane, C. M. Janitzek, S. Matondo, M. Resende, T. Gustavsson, W. A. d. Jongh, S. Clemmensen, W. Roeffen, M. van de Vegte-Bolmer, G. J. van Gemert, R. Sauerwein, J. T. Schiller, M. A. Nielsen, T. G. Theander, A. Salanti, A. F. Sander, *J. Nanobiotechnol.* **2016**, *14*, 30; j) H. B. van Berg Saparoea, D. Houben, M. I. d. Jonge, W. S. P. Jong, J. Luirink, *Appl. Environ. Microbiol.* **2018**, *84*; k) S. Gallus, E. Mittmann, K. S. Rabe, *ChemBioChem* **2022**, *23*, e202100472; l) C. N. Bedbrook, M. Kato, S. Ravindra Kumar, A. Lakshmanan, R. D. Nath, F. Sun, P. W. Sternberg, F. H. Arnold, V. Gradinaru, *Chem. Biol.* **2015**, *22*, 1108–1121; m) H. Moon, Y. Bae, H. Kim, S. Kang, *Chem. Commun.* **2016**, *52*, 14051–14054; n) V. Pessino, Y. R. Citron, S. Feng, B. Huang, *ChemBioChem* **2017**, *18*, 1492–1495; o) M. Pröschel, R. Detsch, A. R. Boccaccini, U. Sonnewald, *Front. Bioeng. Biotechnol.* **2015**, *3*, 168; p) B. Zakeri, *ChemBioChem* **2015**, *16*, 2277–2282.
- [15] N. S. Sarai, B. J. Levin, J. M. Roberts, D. E. Katsoulis, F. H. Arnold, *ACS Cent. Sci.* **2021**, *7*, 944–953.
- [16] H. T. Imam, P. C. Marr, A. C. Marr, *Green Chem.* **2021**, *23*, 4980–5005.
- [17] C. Hentrich, S. J. Kellmann, M. Putyrski, M. Cavada, H. Hanuschka, A. Knappik, F. Ylera, *Cell Chem. Biol.* **2021**, *28*, 813–824.e816.
- [18] G. R. Morrison, *Anal. Chem.* **1965**, *37*, 1124–1126.
- [19] A. J. Pineda-Knauseder, D. A. Vargas, R. Fasan, *Biotechnol. Appl. Biochem.* **2020**, *67*, 516–526.
- [20] H. Renata, R. D. Lewis, M. J. Sweredoski, A. Moradian, S. Hess, Z. J. Wang, F. H. Arnold, *J. Am. Chem. Soc.* **2016**, *138*, 12527–12533.
- [21] E. Arslan, H. Schulz, R. Zufferey, P. Künzler, L. Thöny-Meyer, *Biochem. Biophys. Res. Commun.* **1998**, *251*, 744–747.
- [22] J. von Seckendorff, O. Hinrichsen, *Can. J. Chem. Eng.* **2021**, *99*, S703–S733.

Manuscript received: January 20, 2023

Revised manuscript received: March 17, 2023

Accepted manuscript online: March 21, 2023

Version of record online: April 13, 2023